DALTON
FULL PAPER

Structural and magnetic properties of $Co_3(dpa)_4Br_2$ †

Rodolphe Clérac,[a] F. Albert Cotton,*[a] Lee M. Daniels,[a] Kim R. Dunbar,[a] Carlos A. Murillo *[a,b] and Xiaoping Wang[a]

[a] *Laboratory for Molecular Structure and Bonding, Department of Chemistry, Texas A&M University, PO Box 30012, College Station, TX 77842-3012, USA*
[b] *Department of Chemistry, University of Costa Rica, Ciudad Universitaria, Costa Rica*

Received 28th September 2000, Accepted 30th November 2000
First published as an Advance Article on the web 29th January 2001

Eleven crystal structures have been determined for the trinuclear $Co_3(dpa)_4Br_2$ (**1**) (dpa = di(2-pyridyl)amide anion) molecule in the following solvates: **1**·CH_2Cl_2 (at 111, 147 and 240 K), **1**·C_6H_{12} (at 110, 150, 213 and 298 K) and **1**·$1.75C_7H_8$·$0.5C_6H_{14}$ (at 110, 170, 213 and 295 K). Their magnetic behavior has been measured over the temperature range 5–350 K. In nearly every respect their behavior closely parallels that of their chloro analogs, although certain crystallographic and magnetic details differ. Of particular importance is that both symmetrical and unsymmetrical structures are observed in different crystalline forms and that the unsymmetrical forms display marked temperature dependence. It is, therefore, clear that the highly unconventional behavior of the chloro analog is not restricted to that one compound.

Introduction

Beginning in 1994 $Co_3(dpa)_4X_2$·*n*Solv. compounds have been reported;[1] here X represents some uninegative anion, *n*Solv. denotes *n* molecules of solvent, and dpa is the di(2-pyridyl)-amide ion. Several studies[1] have addressed the unusual structural and magnetic properties of these compounds. Major interest has centered on the compounds with X = Cl. Depending on both the solvent content of the crystals and the temperature, the Co_3 chain in the center of this molecule may vary from being perfectly symmetrical (or very nearly so) through various intermediate stages, to being extremely unsymmetrical. In symmetrical cases both Co–Co distances are *ca.* 2.32 Å while in the extremely unsymmetrical cases, the two Co–Co separations are *ca.* 2.30 Å and *ca* 2.47 Å. This uncommon phenomenon naturally raises the question of whether such variations in the metal-to-metal distances are restricted to an isolated example for X = Cl or if such behavior occurs more generally. Thus the purpose of the work described here was to see whether the analogous $Co_3(dpa)_4Br_2$·*n*Solv. compounds would display the same structural variability and similar magnetic behavior.

Results and discussion

The preparation of $Co_3(dpa)_4Br_2$ is easily accomplished, in 55–60% yield, by the same procedure as we have previously reported[1c] for $Co_3(dpa)_4Cl_2$. It is very important, however, to recognize that the reagents used must be completely free of chloride ion. Otherwise one obtains some $Co_3(dpa)_4BrCl$ and even some $Co_3(dpa)_4Cl_2$. As will be shown later, Cl^- has a strong tendency to replace Br^- in pure $Co_3(dpa)_4Br_2$.

One major difference between $Co_3(dpa)_4Cl_2$ and $Co_3(dpa)_4Br_2$ is that while the former forms two sorts of crystals, one symmetrical s-$Co_3(dpa)_4Cl_2$·CH_2Cl_2 and one unsymmetrical u-$Co_3(dpa)_4Cl_2$·$2CH_2Cl_2$ when crystallized from dichloromethane,[1f] we have not seen any evidence of u-$Co_3(dpa)_4Br_2$·CH_2Cl_2 crystals. The only crystals (Tables 1 and 2 and Fig. 1) we have obtained so far from CH_2Cl_2 are s-$Co_3(dpa)_4Br_2$·CH_2Cl_2.

In the crystals of s-$Co_3(dpa)_4Br_2$·CH_2Cl_2 (space group *Pnn*2, *Z* = 2) the molecule lies on a 2-fold symmetry axis which makes the two Co–Co bonds equivalent. This space group is correct at temperatures of 111, 147 and 240 K, whereas for the analogous $Co_3(dpa)_4Cl_2$·CH_2Cl_2, there was a phase change below room temperature to *Pn*, which simply involved a change from disordered to ordered CH_2Cl_2 molecules and had no significant effect on the structure of the $Co_3(dpa)_4Cl_2$ molecule. Evidently the CH_2Cl_2 molecules in $Co_3(dpa)_4Br_2$·CH_2Cl_2 remain disordered down to at least 111 K.

For $Co_3(dpa)_4Br_2$·C_6H_{12} the crystals are in space group *P*2/*n* at 110, 150, 213 and 298 K (Tables 3 and 4 and Fig. 2). This contrasts with the behavior of the chlorine analog[1h] where the space group was *Pccn* at 295 and 213 K but changed to $P2_1/c$ between 213 and 120 K. It is not to be considered as surprising that the bromo and chloro compounds are not isomorphous considering that the van der Waals radii of Cl (1.80 Å) and Br (1.95 Å) are quite different, and the bromo molecule is thus 0.30 Å longer than its chloro analog. It should be noted that the complex lies on a two-fold axis so that the Co–Co distances must be equivalent.

We previously[1h] commented on the fact that the Co–Co distances in $Co_3(dpa)_4Cl_2$·C_6H_{12} are very sensitive to temperature, increasing by 0.043 Å between 120 and 295 K. An even larger increase is observed in the bromide (0.064 Å).

Turning now to $Co_3(dpa)_4Br_2$·$1.75C_7H_8$·$0.5C_6H_{14}$, for which there is also a chloro analog,[1h] the results are presented in Tables 5 and 6, and Fig. 3. The two compounds are isomorphous (space group $P\bar{1}$, *Z* = 4) and in each one there are two crystallographically independent molecules. The same situation prevailed in the chloro analog. Once again, these two molecules show different behavior as a function of temperature. In the present case the details are as follows. One of the molecules is practically symmetrical at 110 K (Co–Co = 2.317(1) and 2.316(1) Å) but becomes quite unsymmetrical (2.323(1) and 2.433(1) Å) at 295 K. The other molecule is distinctly unsymmetrical even at 110 K (2.310(1) and 2.389(1) Å) and becomes very unsymmetrical at 295 K (2.312(1) and 2.469(1) Å).

---

† Electronic supplementary information (ESI) available: UV-Vis spectra in CH_2Cl_2 and plots of magnetic properties for $Co_3(dpa)_4X_2$ (X = Br or Cl). See http://www.rsc.org/suppdata/dt/b0/b007876j/

DOI: 10.1039/b007876j

Table 1 Crystal data and structure refinement for $Co_3(dpa)_4Br_2{\cdot}CH_2Cl_2$ ($\mathbf{1}{\cdot}CH_2Cl_2$)

Empirical formula		$C_{41}H_{34}N_{12}Co_3Cl_2Br_2$	
FW		1102.31	
Crystal system	Orthorhombic	Orthorhombic	Orthorhombic
Space group	*Pnn*2	*Pnn*2	*Pnn*2
a/Å	12.829(1)	12.849(2)	12.953(1)
b/Å	13.935(2)	13.956(2)	14.055(1)
c/Å	11.158(1)	11.175(2)	11.264(1)
V/Å^3	1994.7(4)	2003.9(6)	2050.7(3)
Z	2	2	2
T/K	111	147	240
d_{calcd}/g cm^{-3}	1.835	1.827	1.785
μ/mm^{-1} (Mo-Kα)	3.420	3.405	3.327
R indices [$I > 2\sigma(I)$], $R1$,[a] $wR2$[b]	0.059, 0.177	0.060, 0.166	0.047, 0.137
R indices (all data), $R1$,[a] $wR2$[b]	0.062, 0.180	0.068, 0.175	0.056, 0.144

[a] $R1 = \Sigma||F_o| - |F_c||/\Sigma|F_o|$. [b] $wR2 = [\Sigma[w(F_o^2 - F_c^2)^2]/\Sigma[w(F_o^2)^2]]^{\frac{1}{2}}$.

Table 2 Selected bond distances (Å) and angles (°) for $\mathbf{1}{\cdot}CH_2Cl_2$

	111 K	147 K	240 K
Co(1)–Co(2)	2.3164(8)	2.3182(8)	2.3234(6)
Co(1)–Br(1)	2.622(1)	2.626(1)	2.6648(9)
Co(1)–N(1)	1.978(6)	1.983(6)	1.995(5)
Co(1)–N(2)	1.973(7)	1.976(6)	1.988(5)
Co(1)–N(3)	1.957(6)	1.968(6)	1.972(5)
Co(1)–N(4)	1.992(7)	2.002(6)	2.005(5)
Co(2)–N(5)	1.880(7)	1.881(7)	1.896(6)
Co(2)–N(6)	1.914(7)	1.919(7)	1.908(6)
Co(1)–Co(2)–Co(1A)	176.7(1)	176.9(1)	177.66(9)
Co(2)–Co(1)–Br(1)	178.15(6)	178.24(5)	178.64(4)
N(1)–Co(1)–N(2)	89.6(3)	89.8(3)	89.7(2)
N(1)–Co(1)–N(3)	89.3(3)	89.3(2)	89.5(2)
N(1)–Co(1)–N(4)	169.9(3)	169.9(2)	170.0(2)
N(2)–Co(1)–N(3)	172.2(3)	172.2(2)	171.6(2)
N(2)–Co(1)–N(4)	90.8(3)	90.3(3)	90.1(2)
N(3)–Co(1)–N(4)	88.9(2)	89.1(2)	89.3(2)
N(1)–Co(1)–Br(1)	94.9(2)	94.9(2)	94.75(14)
N(2)–Co(1)–Br(1)	93.5(2)	93.7(2)	93.88(14)
N(3)–Co(1)–Br(1)	94.3(2)	94.1(2)	94.52(14)
N(4)–Co(1)–Br(1)	95.1(2)	95.2(2)	95.27(14)
N(5A)–Co(2)–N(5)	89.1(4)	89.2(4)	89.3(3)
N(5A)–Co(2)–N(6)	178.3(4)	178.5(3)	179.1(3)
N(5)–Co(2)–N(6)	89.6(2)	89.7(2)	89.9(2)
N(5)–Co(2)–N(6A)	178.3(4)	178.5(3)	179.1(3)
N(6)–Co(2)–N(6A)	91.7(4)	91.3(4)	90.9(4)

Symmetry transformations used to generate equivalent atoms: (A) $-x + 2, -y, z$.

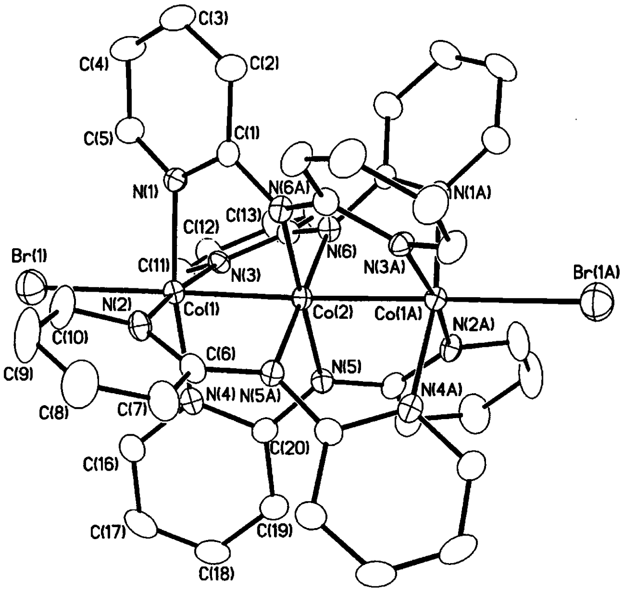

Fig. 1 Perspective view of **1** in $\mathbf{1}{\cdot}CH_2Cl_2$ at 240 K. Atoms are drawn at the 40% probability level and hydrogen atoms are omitted for clarity.

Electrochemistry

As shown in Fig. 4, in CH_2Cl_2 solution, the $Co_3(dpa)_4Br_2$ molecule can be reversibly oxidized at $E_{\frac{1}{2}} = 0.35$ V and 1.25 V. These potentials are essentially the same as those reported[2] for the chloro analog. It should, therefore, be possible to isolate compounds containing the $[Co_3(dpa)_4Br_2]^+$ ion. In view of the very unusual observation of a two-step spin crossover in the analogous chloro cation, we plan to undertake the preparation and study of such compounds.

^{1}H NMR Spectrum

We noted earlier that careful exclusion of chloride in preparing and handling $Co_3(dpa)_4Br_2$ is essential because chlorine readily replaces bromine. Conversely, however, when the product is contaminated by chlorine, it can be displaced by treatment of a solution of contaminated material with a large excess of $(NBu^n{}_4)Br$. This process is shown in Fig. 5, where we begin, at the bottom, with a sample of the chloro compound in the presence of a 50-fold excess of $(NBu^n{}_4)Br$ in CD_2Cl_2. Over a period of 4–5 days at room temperature all chlorine is finally displaced and signals for $Co_3(dpa)_4Cl_2$ and $Co_3(dpa)_4ClBr$ disappear.

It can be seen that the spectrum of the $Co_3(dpa)_4Br_2$ molecule with four types of signals is very similar to that of $Co_3(dpa)_4Cl_2$ and can be assigned in the same way.[1e] For the mixed compound, $Co_3(dpa)_4ClBr$, the number of NMR signals is doubled to a total of eight.

Magnetic properties

The results of the magnetic measurements on $Co_3(dpa)_4Br_2{\cdot}CH_2Cl_2$ are shown in Fig. 6. Those for the chloro analog, which were previously analyzed in detail,[1f] are also plotted to make comparison easy. As in the case of the chloro compound, we have a ground state with $S = \frac{1}{2}$ and a g value of *ca.* 2.35 and then, beginning around 200 K a spin state equilibrium with a higher spin state ($S = \frac{3}{2}$ or $\frac{5}{2}$) begins to manifest itself. Clearly, in the bromo compound the higher spin-state is further above the ground state than in the chloro case. However, it is impossible to be sure whether it has $S = \frac{3}{2}$ or $S = \frac{5}{2}$. In the chloro case, the $S = \frac{5}{2}$ was marginally favored, but a decision here would be impossible because the crystals lose interstitial solvent at temperatures above *ca.* 350 K.

Concluding remarks

This study shows that $Co_3(dpa)_4Br_2$ is very similar to its chloro analog. Thus $Co_3(dpa)_4Cl_2$ is not the *only* case in which the Co–Co distances along the Co_3 chain are equal in some crystals and very unequal in others. However, there is one significant difference that came to light. While the spin-crossover process in s-$Co_3(dpa)_4Br_2{\cdot}CH_2Cl_2$ is quite similar to that in the chloro

Table 3 Crystal data and structure refinement for $Co_3(dpa)_4Br_2\cdot C_6H_{12}$ ($\mathbf{1}\cdot C_6H_{12}$)

Empirical formula	$C_{46}H_{44}N_{12}Co_3Br_2$			
FW	1101.54			
Crystal system	Monoclinic	Monoclinic	Monoclinic	Monoclinic
Space group	*P*2/*n*	*P*2/*n*	*P*2/*n*	*P*2/*n*
a/Å	12.9949(5)	13.0105(7)	13.0226(6)	13.0483(7)
b/Å	11.5683(5)	11.5955(6)	11.6749(5)	11.7668(6)
c/Å	14.2818(6)	14.3119(7)	14.3720(7)	14.4367(8)
β/°	94.229(1)	94.178(1)	93.958(1)	93.781(1)
V/Å^3	2141.1(2)	2153.4(2)	2179.9(2)	2211.7(2)
Z	2	2	2	2
T/K	110	150	213	298
d_{calcd}/g cm^{-3}	1.709	1.699	1.678	1.657
μ/mm^{-1} (Mo-Kα)	3.066	3.048	3.011	2.968
R indices [$I > 2\sigma(I)$], $R1$,[a] $wR2$[b]	0.024, 0.060	0.025, 0.064	0.026, 0.066	0.029, 0.073
R indices (all data), $R1$,[a] wR[b]	0.031, 0.063	0.034, 0.068	0.040, 0.071	0.053, 0.081

[a] $R1 = \Sigma||F_o| - |F_c||/\Sigma|F_o|$. [b] $wR2 = [\Sigma[w(F_o^2 - F_c^2)^2]/\Sigma[w(F_o^2)^2]]^{\frac{1}{2}}$.

Table 4 Selected bond distances (Å) and angles (°) for $Co_3(dpa)_4Br_2\cdot C_6H_{12}$ ($\mathbf{1}\cdot C_6H_{12}$)[a]

	110 K	150(2) K	213(2) K	298(2) K
Co(1)–Co(2)	2.3188(2)	2.3262(3)	2.3566(3)	2.3830(3)
Co(1)–Br(1)	2.6227(3)	2.6187(3)	2.5928(4)	2.5689(4)
Co(1)–N(1)	1.984(2)	1.993(2)	2.020(2)	2.047(2)
Co(1)–N(3)#1	1.9969(15)	2.006(2)	2.033(2)	2.057(2)
Co(1)–N(4)	1.995(2)	2.005(2)	2.034(2)	2.056(2)
Co(1)–N(6)#1	1.987(2)	1.995(2)	2.022(2)	2.044(2)
Co(2)–N(2)	1.895(2)	1.897(2)	1.904(2)	1.909(2)
Co(2)–N(5)	1.890(2)	1.891(2)	1.896(2)	1.899(2)
Co(1)–Co(2)–Co(1)#1	180.00(2)	179.93(2)	179.91(2)	179.95(2)
Co(2)–Co(1)–Br(1)	179.475(11)	179.51(2)	179.48(1)	179.48(2)
N(1)–Co(1)–N(3)#1	89.48(6)	89.49(7)	89.10(7)	88.65(8)
N(1)–Co(1)–N(4)	89.00(6)	88.97(6)	88.82(7)	88.75(8)
N(1)–Co(1)–N(6)#1	170.11(6)	169.65(6)	167.86(7)	166.14(7)
N(3)#1–Co(1)–N(4)	169.16(6)	168.63(6)	166.86(7)	165.26(7)
N(6)#1–Co(1)–N(3)#1	89.50(6)	89.41(6)	89.35(7)	89.16(8)
N(6)#1–Co(1)–N(4)	90.16(6)	90.08(6)	89.96(7)	89.90(8)
N(1)–Co(1)–Br(1)	95.36(4)	95.58(4)	96.48(5)	97.40(7)
N(3)#1–Co(1)–Br(1)	95.54(4)	95.83(4)	96.75(5)	97.56(5)
N(4)–Co(1)–Br(1)	95.29(4)	95.93(4)	96.37(5)	97.16(5)
N(6)#1–Co(1)–Br(1)	94.53(4)	94.77(4)	95.66(5)	96.14(6)
N(2)–Co(2)–N(2)#1	90.76(9)	90.7(1)	90.6(1)	90.3(1)
N(5)–Co(2)–N(2)	89.82(7)	89.88(7)	89.85(7)	89.98(8)
N(5)–Co(2)–N(2)#1	179.21(6)	179.20(7)	179.21(7)	179.34(8)
N(5)#1–Co(2)–N(5)	89.62(9)	89.6(1)	89.7(1)	89.7(1)

[a] Symmetry transformation used to generate equivalent atoms: #1 $-x + \frac{3}{2}, y, -z + \frac{1}{2}$.

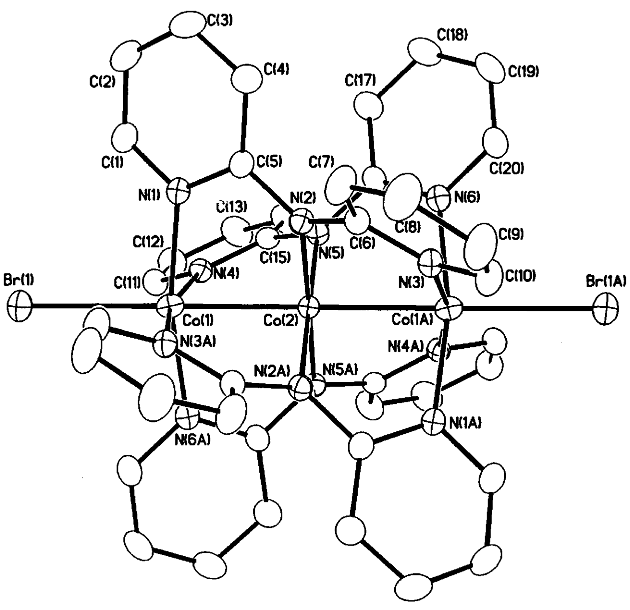

Fig. 2 Perspective view of **1** in $\mathbf{1}\cdot C_6H_{12}$ at 213 K. Atoms are drawn at the 40% probability level and hydrogen atoms are omitted for clarity.

compound, the promotion energy to the higher spin state is somewhat higher. In solution the bromo compound, like its chloro analog, appears to exist in symmetrical form, and in its several solvated crystalline forms the crystals are very similar to, but not always strictly isomorphous with those of the chloro compound. It is therefore not entirely surprising that no u-$Co_3(dpa)_4Br_2\cdot 2CH_2Cl_2$ phase was observed (which, of course, doesn't prove that it doesn't exist). The results presented here provide hope of finding other systems that would shed more light on understanding the factors that affect the Co–Co separations and the related magnetic behavior. By learning how to manipulate the Co_3 chains interesting applications could eventually be developed.

Experimental

Materials

Manipulations were performed under an atmosphere of argon using standard Schlenk techniques. Solvents were purified by conventional methods and were freshly distilled under nitrogen prior to use. Anhydrous cobalt bromide was purchased from Strem Chemicals, Inc.; solutions of methyllithium (as a complex with lithium bromide in diethyl ether) and 2,2′-dipyridylamine were purchased from Aldrich.

Physical measurements

^1H NMR spectra were recorded on a Varian UNITY Plus 300 instrument at 300 MHz, with chemical shifts referenced to CD_2Cl_2 (δ 5.32). IR spectra were recorded on a Perkin-Elmer 16PC FT-IR spectrometer by using KBr pellets. UV-Visible spectra in CH_2Cl_2 solution were recorded on a Cary 17D and are included in the supplementary material.† Cyclic voltammetry was performed in dichloromethane solution with a BAS model 100 scanning potentiostat using Pt working and auxiliary electrodes and 0.1 M TBAH, $(NBu^n_4)PF_6$, as the supporting electrolyte. Potentials are referenced to the ferrocene/ferrocenium (Fc/Fc^+) couple which occurs at $E_{\frac{1}{2}} = +0.44$ V *versus* Ag/AgCl. The values of $E_{\frac{1}{2}}$ were taken as $(E_{pa} + E_{pc})/2$ where E_{pa} and E_{pc} are the anodic and cathodic peak potentials, respectively. The magnetic susceptibility data were collected on a Quantum Design, model MPMS, SQUID housed in the Department of Chemistry at Texas A&M University; data were collected from 1.8 to 350 K at a field of 1000 G.

Syntheses

$\mathbf{1}\cdot CH_2Cl_2$. A solution of Li(dpa) (4.0 mmol) was prepared by adding 2.7 cm^3 of 1.5 M LiMe (4.1 mmol) into a flask con-

Table 5 Crystal data and structure refinement for $\mathbf{1}\cdot1.75C_7H_8\cdot0.5C_6H_{14}$

FW	1221.71			
Crystal system	Triclinic	Triclinic	Triclinic	Triclinic
Space group	$P\bar{1}$	$P\bar{1}$	$P\bar{1}$	$P\bar{1}$
a/Å	16.835(1)	16.927(1)	17.007(1)	17.200(5)
b/Å	18.060(1)	18.155(1)	18.228(1)	18.383(6)
c/Å	19.243(1)	19.293(1)	19.321(1)	19.385(6)
α/°	81.636(2)	81.395(1)	81.220(1)	81.049(6)
β/°	82.881(2)	82.475(2)	82.232(1)	82.046(7)
γ/°	62.516(1)	62.438(1)	62.441(1)	62.464(5)
V/Å^3	5027.6(5)	5183.9(6)	5232.1(7)	5354(3)
Z	4	4	4	4
T/K	110	170	213	295
d_{calcd}/g cm^{-3}	1.583	1.565	1.551	1.516
μ/mm^{-1} (Mo-Kα)	2.571	2.541	2.518	2.461
R indices [$I > 2\sigma(I)$], $R1$,[a] $wR2$[b]	0.048, 0.116	0.049, 0.116	0.052, 0.112	0.053, 0.113
R indices (all data), $R1$,[a] $wR2$[b]	0.088, 0.131	0.099, 0.135	0.117, 0.139	0.132, 0.135

[a] $R1 = \Sigma||F_o| - |F_c||/\Sigma|F_o|$. [b] $[\Sigma[w(F_o^2 - F_c^2)^2]/\Sigma[w(F_o^2)^2]]^{\frac{1}{2}}$.

Table 6 Selected interatomic distances (Å) and angles (°) for $\mathbf{1}\cdot1.75C_7H_8\cdot0.5C_6H_{14}$

	110 K	170 K	213 K	295 K		110 K	170 K	213 K	295 K
Molecule A									
Co(1)–Co(2)	2.3097(9)	2.3062(9)	2.3052(10)	2.3123(13)	Co(2)–N(2)	1.897(3)	1.901(4)	1.904(4)	1.901(5)
Co(2)–Co(3)	2.3892(9)	2.4313(9)	2.4512(10)	2.4690(13)	Co(2)–N(5)	1.902(3)	1.904(3)	1.900(4)	1.911(5)
Co(1)–Br(1)	2.5877(8)	2.5887(9)	2.5874(10)	2.5935(13)	Co(2)–N(8)	1.905(3)	1.910(4)	1.911(4)	1.911(5)
Co(3)–Br(2)	2.6259(8)	2.5800(9)	2.5566(10)	2.5456(13)	Co(2)–N(11)	1.897(3)	1.898(3)	1.902(4)	1.911(5)
Co(1)–N(1)	1.976(4)	1.965(4)	1.972(4)	1.984(5)	Co(3)–N(3)	2.040(4)	2.075(4)	2.092(4)	2.116(5)
Co(1)–N(4)	1.974(4)	1.973(4)	1.973(4)	1.972(5)	Co(3)–N(6)	2.039(3)	2.088(4)	2.108(4)	2.123(5)
Co(1)–N(7)	1.979(4)	1.976(4)	1.974(4)	1.985(6)	Co(3)–N(9)	2.047(3)	2.074(4)	2.089(4)	2.110(5)
Co(1)–N(10)	1.985(4)	1.980(4)	1.984(4)	1.984(5)	Co(3)–N(12)	2.042(4)	2.079(4)	2.097(4)	2.119(5)
Co(1)–Co(2)–Co(3)	178.72(3)	178.24(3)	178.02(4)	178.05(5)	N(6)–Co(3)–N(3)	90.05(14)	89.26(14)	88.69(15)	88.3(2)
Co(2)–Co(1)–Br(1)	179.71(3)	179.80(4)	179.83(4)	179.89(4)	N(3)–Co(3)–N(9)	92.53(14)	92.91(14)	92.8(2)	92.2(2)
Co(2)–Co(3)–Br(2)	178.60(3)	179.18(3)	179.39(4)	179.63(4)	N(3)–Co(3)–N(12)	167.3(2)	164.6(2)	163.2(2)	162.2(2)
N(4)–Co(1)–N(1)	89.95(14)	90.1(2)	89.8(2)	90.0(2)	N(6)–Co(3)–N(9)	167.34(15)	164.7(2)	163.6(2)	162.4(2)
N(1)–Co(1)–N(7)	90.12(15)	90.0(2)	89.9(2)	90.0(2)	N(6)–Co(3)–N(12)	84.52(13)	83.75(14)	83.89(15)	83.8(2)
N(1)–Co(1)–N(10)	170.6(2)	170.9(2)	170.8(2)	170.6(2)	N(12)–Co(3)–N(9)	90.38(14)	90.36(14)	90.2(2)	90.6(2)
N(4)–Co(1)–N(7)	170.9(2)	170.8(2)	170.8(2)	169.8(2)	N(1)–Co(1)–Br(1)	93.99(11)	93.82(12)	94.25(13)	94.2(2)
N(4)–Co(1)–N(10)	87.83(14)	88.0(2)	88.3(2)	88.5(2)	N(4)–Co(1)–Br(1)	95.07(11)	95.22(12)	95.16(13)	95.6(2)
N(7)–Co(1)–N(10)	90.63(14)	90.6(2)	90.4(2)	89.9(2)	N(7)–Co(1)–Br(1)	93.98(12)	93.99(13)	94.06(14)	94.6(2)
N(2)–Co(2)–N(5)	89.52(15)	89.5(2)	89.4(2)	89.3(2)	N(10)–Co(1)–Br(1)	95.33(11)	95.16(12)	94.91(13)	95.1(2)
N(2)–Co(2)–N(8)	90.40(15)	90.6(2)	90.8(2)	90.7(2)	N(3)–Co(3)–Br(2)	95.81(11)	96.93(11)	97.82(12)	97.9(2)
N(11)–Co(2)–N(2)	179.3(2)	179.2(2)	179.1(2)	179.3(2)	N(6)–Co(3)–Br(2)	97.22(10)	98.46(11)	99.02(11)	99.74(14)
N(5)–Co(2)–N(8)	179.3(2)	179.3(2)	178.8(2)	178.6(2)	N(9)–Co(3)–Br(2)	94.85(11)	96.35(11)	97.00(12)	97.6(2)
N(11)–Co(2)–N(5)	89.81(14)	89.8(2)	90.0(2)	90.1(2)	N(12)–Co(3)–Br(2)	96.30(11)	97.63(12)	98.19(12)	99.2(2)
N(11)–Co(2)–N(8)	90.26(15)	90.0(2)	89.8(2)	89.9(2)					
Molecule B									
Co(4)–Co(5)	2.3173(8)	2.3118(8)	2.3099(9)	2.3234(13)	Co(5)–N(14)	1.907(3)	1.887(4)	1.892(4)	1.892(5)
Co(5)–Co(6)	2.3162(8)	2.3536(9)	2.3917(10)	2.4333(13)	Co(5)–N(17)	1.883(4)	1.906(3)	1.908(4)	1.913(4)
Co(4)–Br(3)	2.5861(7)	2.6226(8)	2.6158(9)	2.6065(13)	Co(5)–N(20)	1.892(3)	1.890(4)	1.887(4)	1.903(5)
Co(6)–Br(4)	2.6288(7)	2.5632(8)	2.5350(9)	2.5090(13)	Co(5)–N(23)	1.888(4)	1.897(3)	1.902(4)	1.915(4)
Co(4)–N(13)	1.978(3)	2.008(4)	2.007(4)	2.021(5)	Co(6)–N(15)	1.966(3)	2.016(4)	2.045(4)	2.079(5)
Co(4)–N(16)	1.977(4)	1.968(4)	1.974(4)	1.989(5)	Co(6)–N(18)	2.012(4)	2.013(4)	2.048(4)	2.083(5)
Co(4)–N(19)	2.043(3)	1.982(4)	1.976(4)	1.991(5)	Co(6)–N(21)	1.988(3)	2.015(4)	2.055(4)	2.096(5)
Co(4)–N(22)	1.981(4)	1.986(4)	1.979(4)	1.991(5)	Co(6)–N(24)	1.983(4)	2.070(4)	2.105(4)	2.131(5)
Co(6)–Co(5)–Co(4)	176.48(3)	177.06(3)	177.41(4)	177.93(5)	N(15)–Co(6)–N(18)	89.16(14)	89.05(15)	88.8(2)	88.5(2)
Co(5)–Co(4)–Br(3)	177.10(3)	177.71(3)	177.98(3)	178.28(4)	N(15)–Co(6)–N(21)	170.12(15)	168.4(2)	165.9(2)	163.6(2)
Co(5)–Co(6)–Br(4)	177.39(3)	177.51(4)	177.82(4)	178.40(5)	N(15)–Co(6)–N(24)	90.18(14)	91.77(14)	91.7(2)	91.2(2)
N(16)–Co(4)–N(13)	89.18(14)	89.13(15)	89.3(2)	89.1(2)	N(21)–Co(6)–N(18)	90.80(14)	167.03(15)	87.4(2)	87.5(2)
N(13)–Co(4)–N(19)	169.13(15)	169.2(2)	169.1(2)	168.6(2)	N(24)–Co(6)–N(18)	169.02(15)	87.78(15)	164.9(2)	162.7(2)
N(13)–Co(4)–N(22)	88.09(14)	90.68(15)	90.9(2)	91.1(2)	N(24)–Co(6)–N(21)	87.98(14)	88.84(14)	88.4(2)	88.0(2)
N(16)–Co(4)–N(19)	91.67(14)	90.18(15)	89.7(2)	89.9(2)	N(13)–Co(4)–Br(3)	95.39(10)	94.62(11)	94.68(12)	94.97(15)
N(16)–Co(4)–N(22)	170.44(15)	170.1(2)	170.4(2)	169.6(2)	N(16)–Co(4)–Br(3)	92.67(10)	95.81(11)	95.76(12)	96.11(15)
N(22)–Co(4)–N(19)	89.31(14)	88.15(15)	88.3(2)	88.0(2)	N(19)–Co(4)–Br(3)	95.40(10)	96.18(11)	96.24(12)	96.4(2)
N(17)–Co(5)–N(14)	89.88(15)	90.00(15)	90.0(2)	90.3(2)	N(22)–Co(4)–Br(3)	96.70(11)	94.09(11)	93.82(12)	94.2(2)
N(20)–Co(5)–N(14)	178.64(15)	179.3(2)	179.2(2)	179.3(2)	N(15)–Co(6)–Br(4)	95.82(10)	93.91(11)	95.32(11)	97.02(14)
N(23)–Co(5)–N(14)	90.23(15)	89.75(15)	89.5(2)	89.2(2)	N(18)–Co(6)–Br(4)	94.56(11)	96.40(10)	97.37(11)	98.15(14)
N(17)–Co(5)–N(20)	89.81(15)	90.27(15)	90.4(2)	90.4(2)	N(21)–Co(6)–Br(4)	94.03(10)	97.58(11)	98.60(12)	99.3(2)
N(17)–Co(5)–N(23)	179.3(2)	178.61(15)	178.4(2)	178.0(2)	N(24)–Co(6)–Br(4)	96.41(11)	96.46(11)	97.61(12)	99.1(2)
N(23)–Co(5)–N(20)	90.10(15)	89.99(15)	90.1(2)	90.1(2)					

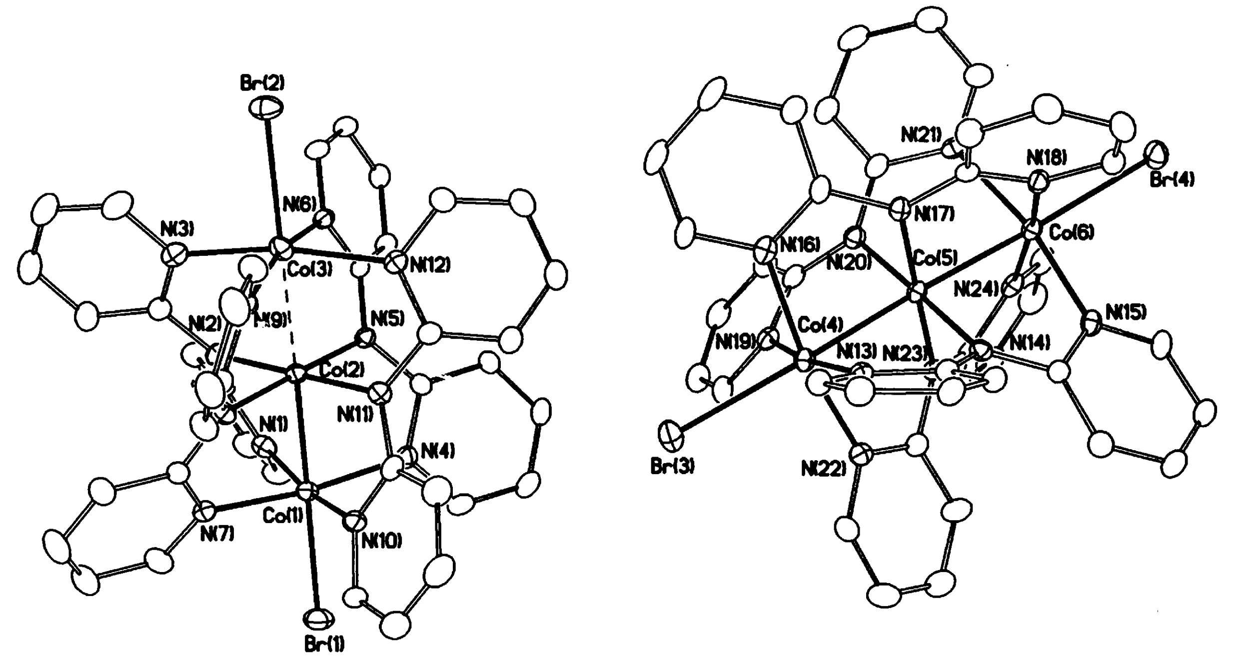

Fig. 3 Perspective view of the two independent molecules of **1** in **1**·1.75C_7H_8·0.5C_6H_{14} at 110 K. Atoms are drawn at the 40% probability level and hydrogen atoms are omitted for clarity. The same atomic labeling scheme is used for data collected at other temperatures.

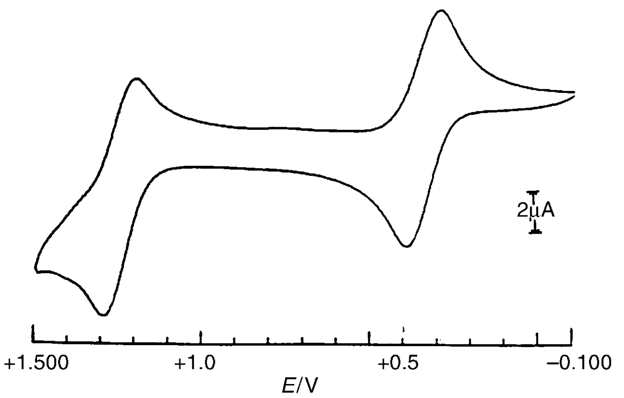

Fig. 4 Cyclic voltammogram (CV) of **1** (3.0×10^{-4} M) in CH_2Cl_2 solution.

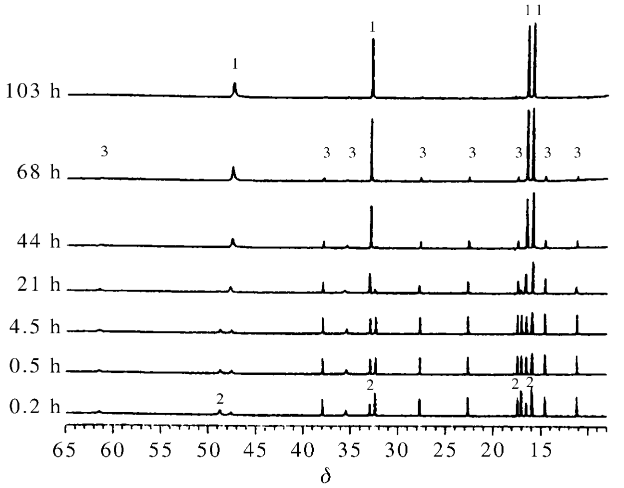

Fig. 5 The time dependence of the ^{1}H NMR spectra of a mixture of $Co_3(dpa)_4Br_2$ (**1**), $Co_3(dpa)_4BrCl$ (**2**) and $Co_3(dpa)_4Cl_2$ (**3**) with the presence of a 50-fold excess of $Bu^n{}_4NBr$ in CD_2Cl_2.

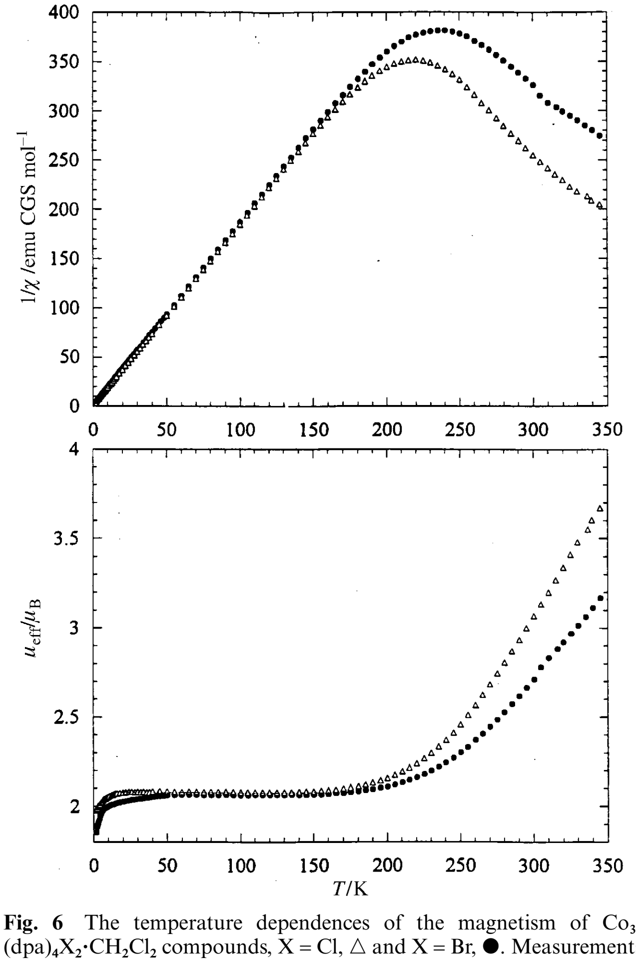

Fig. 6 The temperature dependences of the magnetism of $Co_3(dpa)_4X_2·CH_2Cl_2$ compounds, X = Cl, △ and X = Br, ●. Measurements were made at 1000 G and the TIP corrections were 1.06×10^{-3} and 5.15×10^{-3} emu CGS mol^{-1} for the chloro and bromo compounds, respectively.

taining Hdpa (0.685 g, 4.0 mmol) in 30 cm^3 of THF at −78 °C. The resulting white suspension was allowed to warm slowly to room temperature to give a pale yellow solution. It was then transferred *via* cannula to a reaction flask containing anhydrous $CoBr_2$ (0.66 g, 3.0 mmol). A reddish green suspension was formed in about 15 min. After the mixture was refluxed for 8 h, a dark purple solid was formed. The supernatant solvent was removed by filtration. The remaining solid was washed with ether (15 cm^3), hexanes (15 cm^3), and dried under vacuum to give a brown powder, presumably product **1**. The brown powder was then extracted with CH_2Cl_2 (25 cm^3) and filtered. Dark brown crystals of **1**·CH_2Cl_2 were obtained by slow diffusion of hexanes onto the filtrate in two weeks. Yield 0.63 g, 57%. ^1H NMR (CD_2Cl_2, rt) δ 47.24 (8H), 32.70 (8H), 16.40 (8H), 15.88 (8H). IR (cm^{-1}) 1606 (s), 1593 (s), 1547 (w), 1470 (s), 1428 (s), 1368 (s), 1317 (m), 1282 (w), 1268 (vw), 1250 (vw), 1167 (w), 1152 (m), 1116 (w), 1022 (m), 927 (vw), 884 (w), 758 (s), 735 (s), 540 (w), 518 (w), 456 (w), 427 (w). $E_{\frac{1}{2}}(ox)_1$ 348 mV, $E_{\frac{1}{2}}(ox)_2$ 1251 mV. Anal. Calcd. for $C_{41}H_{34}N_{12}Br_2Cl_2Co_3$: C, 44.87; H, 3.11; N, 15.25. Found C, 45.33; H, 3.22; N, 15.42%.

1·C_6H_{12}. It was prepared in a way similar to that for the dichloromethane solvate. The product was only slightly soluble in toluene. After layering the toluene solution with cyclohexanes, crystals were obtained in about two weeks. IR (cm^{-1}) 1604 (s), 1594 (s), 1547 (w), 1471 (s), 1427 (s), 1371 (s), 1314 (m), 1283 (m), 1238 (w), 1150 (m), 1054 (w), 1020 (m), 1008(w), 978 (vw), 959 (vw), 926 (vw), 886 (w), 760 (s), 738 (m), 638 (vw), 538 (w), 515 (w), 460 (w), 425 (w).

1·1.75C_7H_8·0.5C_6H_{14}. It was prepared in a way similar to that for the dichloromethane solvate. The product was extracted with toluene and layered with hexanes. Crystals were obtained in about 10 days as thin plates. IR (cm^{-1}) 1605 (s), 1593 (s), 1544 (w), 1468 (s), 1459 (s), 1422 (s, br), 1366 (s), 1313 (m), 1282 (w), 1262 (w), 1153 (s), 1107 (vw), 1053 (vw), 1020 (m), 886 (w), 803 (w), 760 (s), 737 (m), 695 (w), 519 (w), 462 (w), 422 (w).

Structure solution and refinement

In each case, a suitable crystal was attached to the end of a quartz fiber with a small amount of silicone grease and transferred to a goniometer head. Single-crystal X-ray studies of **1**·CH_2Cl_2 at 111 and 147 K were performed on a Nonius CAD4 diffractometer. Detailed procedures have previously been described.[3] Data for **1**·CH_2Cl_2 at 240 K, **1**·C_6H_{12} at 110, 150, 213 and 298 K, and **1**·1.75C_7H_8·0.5C_6H_{14} at 110, 170, 213 and 295 K were collected on a Bruker SMART 1000 CCD detector system equipped with a liquid nitrogen low-temperature controller. Cell parameters were obtained using SMART[4] software. Data were corrected for Lorentz and polarization effects using the program SAINTPLUS.[5] Absorption corrections were applied using SADABS.[6]

For each of the data sets the positions of the heavy atoms were found by the direct methods program in SHELXTL.[7] Subsequent cycles of least-squares refinement followed by difference-Fourier syntheses revealed the positions of the remaining non-hydrogen atoms. The interstitial solvent molecules were found to be disordered in **1**·C_6H_{12} and **1**·1.75C_7H_8·0.5C_6H_{14}. All non-hydrogen atoms except the disordered solvent molecules were refined anisotropically.

CCDC reference number 186/2305.

See http://www.rsc.org/suppdata/dt/b0/b007876j/ for crystallographic files in .cif format.

Acknowledgement

The authors acknowledge financial support from the National Science Foundation.

References

1 (*a*) E.-C. Yang, M.-C. Cheng, M.-S. Tsai and S.-M. Peng, *J. Chem. Soc.*, *Chem. Commun.*, 1994, 2377; (*b*) F. A. Cotton, L. M. Daniels and G. T. Jordan IV, *Chem. Commun.*, 1997, 421; (*c*) F. A. Cotton, L. M. Daniels, G. T. Jordan IV and C. A. Murillo, *J. Am. Chem. Soc.*, 1997, **119**, 10377; (*d*) F. A. Cotton, C. A. Murillo and X. Wang, *J. Chem. Soc.*, *Dalton Trans.*, 1999, 3327; (*e*) F. A. Cotton, C. A. Murillo and X. Wang, *Inorg. Chem.*, 1999, **38**, 6294; (*f*) R. Clérac, F. A. Cotton, L. M. Daniels, K. R. Dunbar, K. Kirschbaum, C. A. Murillo, A. A. Pinkerton, A. J. Schultz and X. Wang, *J. Am. Chem. Soc.*, 2000, **122**, 6226; (*g*) R. Clérac, F. A. Cotton, S. P. Jeffery, C. A. Murillo and X. Wang, *Inorg. Chem.*, in press; (*h*) R. Clérac, F. A. Cotton, L. M. Daniels, K. Dunbar, C. A. Murillo and X. Wang, *Inorg. Chem.*, in press.
2 R. Clérac, F. A. Cotton, K. R. Dunbar, T. Lu, C. A. Murillo and X. Wang, *J. Am. Chem. Soc.*, 2000, **122**, 2272.
3 A. Bino, F. A. Cotton and P. Fanwick, *Inorg. Chem.*, 1979, **18**, 3558.
4 SMART, version 5.05 Software for the CCD Detector System, Bruker Analytical X-ray Systems, Inc., Madison, WI, 1998.
5 SAINTPLUS, version 5.00 Software for the CCD Detector System, Bruker Analytical X-ray Systems, Inc., Madison, WI, 1998.
6 SADABS, Program for absorption correction using SMART CCD based on the method of R. H. Blessing, *Acta Crystallogr.*, *Sect. A*, 1995, **51**, 33.
7 SHELXTL, version 5.03, Siemens Industrial Automation, Inc., Madison, WI, 1994.